ELSEVIER

Journal of Chromatography A, 802 (1998) 3–15

JOURNAL OF CHROMATOGRAPHY A

On-line coupling of partial-filling micellar electrokinetic chromatography with mass spectrometry

Pim G. Muijselaar*, Koji Otsuka, Shigeru Terabe

Faculty of Science, Himeji Institute of Technology, Kamigori, Hyogo 678-12, Japan

Abstract

The on-line coupling of micellar electrokinetic chromatography (MEKC) with mass spectrometry (MS) is hampered by the presence of high concentrations of surfactant in the electrolyte system. Partial-filling MEKC (PF-MEKC) provides a possible way to overcome this problem. In PF-MEKC only a part of the capillary is filled with an electrolyte solution containing micelles, thus allowing an MEKC separation without allowing surfactant to enter the mass spectrometer. The migration behaviour of the micellar zone was investigated applying indirect UV detection. It was demonstrated that micelles gradually break down under PF-MEKC conditions and migrate as surfactant monomers at a concentration at or below the critical micelle concentration. The influence of several experimental parameters on the separation performance is studied and the possibilities as well as the limitations of PF-MEKC are discussed. On-line PF-MEKC–MS with sodium dodecyl sulphate micelles is demonstrated for some pharmaceuticals applying an atmospheric pressure chemical ionisation interface. © 1998 Elsevier Science B.V.

Keywords: Partial-filling micellar electrokinetic chromatography; Micellar electrokinetic chromatography–mass spectrometry; Buffer composition; Defection; Electrophoresis; Alkyl amine ketones; Ketones; Caffeine; Ethenzmide; Surfactants

1. Introduction

Micellar electrokinetic chromatography mass spectrometry (MEKC–MS) is an attractive analytical method to obtain both separation and structural information on various substances in biological and pharmaceutical fields. However, on-line coupling of MEKC with MS is troublesome due to the presence of high concentrations of non-volatile surfactant molecules in the electrolyte system. This results in ion-source contamination, low ionisation efficiencies and loss of detector sensitivity [1,2]. Different strategies have been followed to overcome this problem. Takada et al. [3] described an atmospheric pressure chemical ionisation (APCI) interface for capillary electrophoresis–mass spectrometry. APCI was shown to be less affected than electrospray ionisation (ESI) by high salt concentrations present in the electrolyte system, and was successfully applied for the direct coupling of MEKC–MS [4]. Lamoree et al. [5] used a coupled capillary set-up with a voltage switching and buffer renewal system which allows heartcutting of the sample zones with subsequent transfer via a second capillary to the MS. Ozaki et al. [6] applied a high-molecular-mass surfactant as pseudostationary phase, which does not significantly deteriorate the ionisation efficiency. Nelson et al. [7] and Koezuka et al. [8] reported on partial-filling MEKC (PF-MEKC) for on-line coupling with MS. In PF-MEKC only a part of the capillary is filled with an electrolyte solution containing micelles. After separation has been estab-

*Corresponding author.

0021-9673/98/$19.00
PII S0021-9673(97)01089-3

lished in the micellar zone, separated sample zones migrate in front of this micellar zone towards the detector. Hence this method allows a separation based on micellar solubilization without surfactant entering the mass spectrometer. Recently, Yang et al. [9] described on-line MEKC–MS using an intermediate pH buffer, resulting in a low electroosmotic flow (EOF) and an overall velocity of the micelles towards the anode.

Since sodium dodecyl sulphate (SDS) is the most widely used surfactant in MEKC [10,11], on-line MEKC–MS using SDS as pseudostationary phase is an interesting field with respect to method development. In this work the migration behaviour of SDS micelles under PF-MEKC conditions is investigated. In addition, the influence of several experimental parameters such as sample composition, micelle zone length and surfactant concentration on the separation performance is studied. Finally, the application of on-line PF-MEKC–MS is demonstrated by the separation and identification of some pharmaceuticals.

2. Theory

The principle of PF-MEKC is schematically illustrated in Fig. 1. The capillary is filled with a buffer solution without surfactant. At the inlet side a micellar solution is introduced for a short period, either by hydrodynamic or by electrokinetic injection. Subsequently the sample is injected and the separation voltage is applied. While the sample

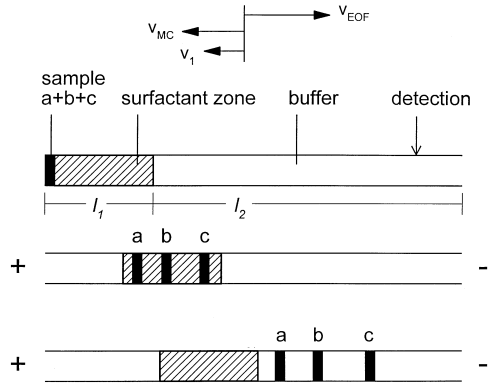

Fig. 1. Schematic representation of the separation mechanism in partial filling MEKC. For further explanation, see text.

compounds migrate in the micelle zone they are separated according to the same mechanism as in normal MEKC [12,13]. After they pass the micelle zone–buffer boundary they migrate in front of the micelle zone towards the detector with the electroosmotic flow. The separation voltage is switched off before the micelle zone reaches the detector. This method has been applied in affinity electrokinetic chromatography with strong UV absorbing pseudostationary phases in order to increase detector sensitivity [14,15]. It has also proven to be useful for the on-line coupling of MEKC–MS with SDS (an anionic surfactant) [7] and sucrose monododecanoate (a non-ionic surfactant) [8] as pseudostationary phases.

In PF-MEKC the surfactant concentration and the micelle zone length are the main experimental parameters that can be varied to change migration times and optimise resolution. In order to demonstrate the influence of these two experimental parameters, an expression was derived for the migration time in PF-MEKC as a function of the retention factor and the micelle zone length (see Fig. 1).

The electroosmotic velocity, ν_{EOF}, and the electrophoretic velocity of the micelles, ν_{MC}, are given by:

$$\nu_{EOF} = \mu_{EOF}E \quad (1)$$

and

$$\nu_{MC} = \mu_{MC}E \quad (2)$$

where μ_{EOF} and μ_{MC} are the electroosmotic mobility and the effective mobility of the micelles, respectively. The electrophoretic velocity of an analyte in the micelle zone, ν_1, is given by:

$$\nu_1 = \frac{k}{1+k}\mu_{MC}E \quad (3)$$

The time during which an analyte will migrate in the micelle zone, t_1, is given by:

$$t_1 = \frac{l_1}{\nu_{MC} - \nu_1} \quad (4)$$

and the migration distance during this time will be:

$$(\nu_1 + \nu_{EOF})t_1. \quad (5)$$

The remaining distance to the detector is:

$$(l_1 + l_2) - (\nu_1 + \nu_{EOF})t_1 \quad (6)$$

and the corresponding migration time, t_2, is:

$$t_2 = \frac{(l_1 + l_2) - (\nu_1 + \nu_{EOF})t_1}{\nu_{EOF}} \quad (7)$$

Hence the total migration time, t_M, can be calculated by:

$$t_M = t_1 + t_2 = \left(\frac{l_1}{\nu_{MC} - \nu_1}\right)\left(1 - \frac{\nu_1 + \nu_{EOF}}{\nu_{EOF}}\right) + \left(\frac{l_1 + l_2}{\nu_{EOF}}\right) \quad (8)$$

Where ν_{EOF}, ν_{MC} and ν_1 are given by Eqs. (1)–(3). In Fig. 2 t_M is shown for different retention factors as a function of the micelle zone length. A linear relationship is obtained up to the migration time of the front of the micelle zone. For higher values of l_1 the migration time does not further increase since the analyte is still migrating in the micellar zone. A longer micelle zone provides a larger separation volume and consequently larger differences in migration times are obtained. However, the front of the micelle zone will reach the detector earlier which reduces the available time window for separation. These two phenomena work opposite each other. The graphs in Fig. 2 suggest that for a given sample mixture there exists a specific micelle zone composition, i.e. surfactant concentration and micelle zone length, where maximum resolution is obtained while the compound with the highest retention factor is still detected before the micelle zone reaches the detector.

Here it should be noted that in this simplified model several assumptions are made. First, differences in the electric field strengths in l_1 (micelle zone) and l_2 (buffer) are neglected. Second, the micelle zone is supposed to stay fully intact during the whole analysis. In practice this is not true, since charged micelles in PF-MEKC gradually break down as will be shown in Section 4.

3. Experimental

3.1. Chemicals and solutions

All chemicals were of analytical-reagent grade and used as received. All SDS solutions for PF-MEKC experiments were prepared in the appropriate background electrolyte. A stock solution of acetophenone, propiophenone and butyrophenone was prepared by dissolving 5 μl of each compound in 10 ml methanol. This solution was diluted 10 times with the buffer electrolyte without SDS unless otherwise noted, giving a final concentration of 0.05 μl ml^{-1}.

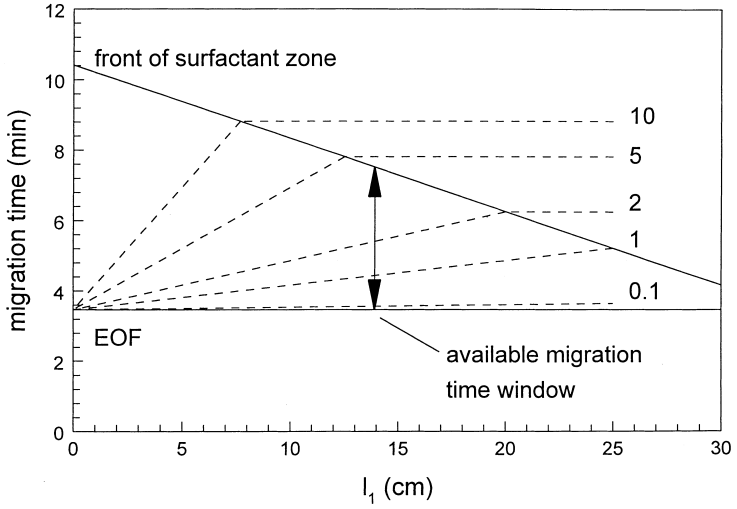

Fig. 2. Calculated migration times as a function of the injected surfactant zone length, l_1, according to Eq. (8), for different retention factors (0.1–10). Solid lines represent the EOF and the front of the surfactant zone, respectively. Model values: capillary length, 50 cm, separation voltage, 20 kV, $\mu_{EOF} = 60 \cdot 10^{-5}$ $cm^2/V\,s$, $\mu_{MC} = -40 \cdot 10^{-5}$ $cm^2/V\,s$.

A stock solution of acetaminophen, caffeine, guaifenisin, ethenzamide and isopropylantipyrine was prepared in methanol at a concentration of 2 mg ml^{-1} for each compound. This solution was diluted 10 times with a 25 m*M* SDS solution, giving a final concentration of 0.2 mg ml^{-1} for each compound. Sample solutions for the MS experiments were prepared by dissolving caffeine and ethenzamide in a 25 m*M* SDS solution at a concentration of 0.5 mg ml^{-1}. Water was purified by a Milli-Q water purification system (Waters Millipore, Milford, MA, USA). All buffer solutions were filtered through 0.45-μm filters prior to use.

3.2. Instrumentation and separation conditions

PF-MEKC experiments with UV and indirect UV detection were performed with an HP^{3D}CE instrument (Hewlett Packard, Waldbronn, Germany) at a constant temperature of 25°C. Multiwavelength detection was carried out at 200, 214 and 245 nm, respectively. A 50 μm I.D.×375 μm O.D. fused-silica capillary (Polymicro Technologies, Phoenix, AZ, USA) was used, total length 64.5 cm, distance between injection and detection, 56.0 cm. The SDS micellar zone was introduced by electrokinetic injection, applying 10 kV. Samples were introduced by a 2-s pressure injection with 50 mbar, unless noted otherwise. For all experiments a constant separation voltage of 20 kV was applied.

On-line PF-MEKC–MS experiments were performed with a Jasco CE 990 (Tokyo, Japan) CE instrument and a Hitachi (Tokyo, Japan) M-1000 quadrupole mass spectrometer, equipped with an APCI interface as described in detail previously [3,4]. This interface was developed for CE–MS with electrolyte systems containing high concentrations of non-volatile salts, including normal MEKC–MS [3,4]. It should be mentioned that PF-MEKC–MS, as described in this paper, can also be carried out using an electrospray ionisation interface [7,8]. In Fig. 3 a schematic representation of the equipment is shown. The interface consists of an electrospray-type nebulizer, a vaporizer and an atmospheric pressure chemical ionization source. The outlet side of the capillary was inserted into the electrospray probe and protruded ~0.5 mm at the probe tip. The electrospray probe was maintained at 3 kV by an external power supply. A sheath liquid of methanol was delivered at 30 μl min^{-1} by a Hitachi L6300 HPLC pump. No drying or nebulizing gas was used. The vaporizer consists of a 60-mm long stainless steel block, uniformly heated to 300°C, with a cylindrical opening of 5 mm I.D. A needle electrode is located between the vaporizer and the first aperture which is maintained at 3 kV to produce a corona discharge. Vaporized sample and solvent molecules are ionised by the corona discharge resulting in ion/molecule reactions [3,4]. The first and second apertures were maintained at 120°C. A drift voltage of 50 V was applied between the first and second apertures for collision induced dissociation of cluster ions. The focusing voltage was set at 110 V, the multiplier voltage was set at 1500 V.

A 50 μm I.D.×150 μm O.D. fused-silica capillary (Polymicro Technologies) was used, total length 100 cm. At 65 cm UV detection was carried out at 214 nm with a Jasco CE 970 UV detector. At this point the capillary was covered by a ~15-cm long, 200 μm I.D.×375 μm O.D fused-silica guide-capillary to focus the separation capillary in the UV detector cell. The SDS surfactant zone was introduced by

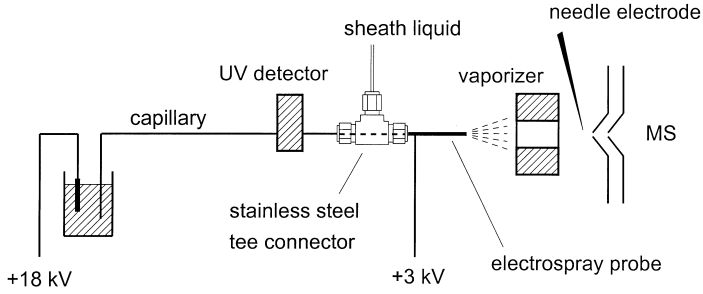

Fig. 3. Schematic representation of the MEKC–APCI-MS equipment.

pressure, applying 200 mbar for 1 min, which resulted in a zone length of ~10 cm. Samples were introduced by pressure injection with 50 mbar for 6 s in the selected ion monitoring mode and for 30 s in the full scan mode. At the inlet side a voltage of 18 kV was applied, resulting in an effective separation voltage of 15 kV. The mass spectrometer was operated in the positive ion mode. In the full scan mode data were collected from m/z 1 to 1000 at 4 s per scan.

4. Results and discussion

4.1. Migration behaviour of the surfactant zone

To describe the separation mechanism in PF-MEKC, a good understanding of the migration behaviour of the surfactant zone is of key importance. Nelson et al. [7,16] applied quinine hydrochloride, a UV-absorbing micelle marker, to monitor the micelle zone in PF-MEKC. In fact this is an indirect method where the migration time of a marker is measured which is assumed to represent the migration time of the injected micelles. However, one should be careful to use such a method since micelles are no rigid spheres and the behaviour of the injected micellar solution in PF- MEKC is not straightforward. A micellar solution is a dynamic system where micelles are in equilibrium with the surrounding aqueous phase, containing individual surfactant molecules [17]. However, the electrophoretic properties of surfactant molecules in the aqueous phase and in the micellar phase are extremely different. Generally micelles possess a much higher effective mobility than the individual surfactant molecules. This is due to the reduction of viscous drag with micelle formation, i.e. a micelle formed by n surfactant molecules experiences less viscous drag than the total viscous drag experienced by n individual surfactant molecules. In Table 1 the effective mobility of dodecyl sulphate (DS) micelles, measured by MEKC and timepidium bromide as micelle marker, and the effective mobility of DS monomers, measured by capillary zone electrophoresis (CZE) with indirect UV-detection, are listed. As expected, a much higher effective mobility is obtained for DS micelles than for individual DS ions.

Table 1
Effective mobility, μ_{eff} (10^{-5} cm^2/V s), of dodecyl sulphate micelles and dodecyl sulphate monomers

DS micelles	−37.40[a]
DS monomers	−20.83[b]

Electrolyte system: 50 m*M* Tris–MES (pH 8.5) containing (a) 25 m*M* and (b) 0 m*M* SDS.
Sample: (a) 1 m*M* timepidium bromide (micelle marker) dissolved in 25 m*M* SDS and (b) 2.5 m*M* SDS dissolved in water.

Hence both the electrophoretic migration of micelles and of surfactant monomers in the aqueous phase have to be considered to describe the migration behaviour of the surfactant zone in PF-MEKC.

In order to elucidate the migration behaviour of DS micelles in PF-MEKC, experiments were carried out with a UV absorbing electrolyte system of 50 m*M* Tris adjusted to pH 8.5 by adding 2-(N-morpholino)ethanesulphonic acid (MES). With this electrolyte system the DS ions, both as micelles and as surfactant monomers, can be monitored by indirect UV detection with MES as visualising agent. In Fig. 4A the electropherogram is shown for the electrokinetic injection (10 kV, 10 s) of 25 m*M* SDS, dissolved in background electrolyte. The non-UV-absorbing positive sodium ions can be observed as a positive peak. According to the Kohlrausch regulation function, the total ionic concentration of a compound in a sample zone is higher than that of the co-ion of the background electrolyte, if its effective

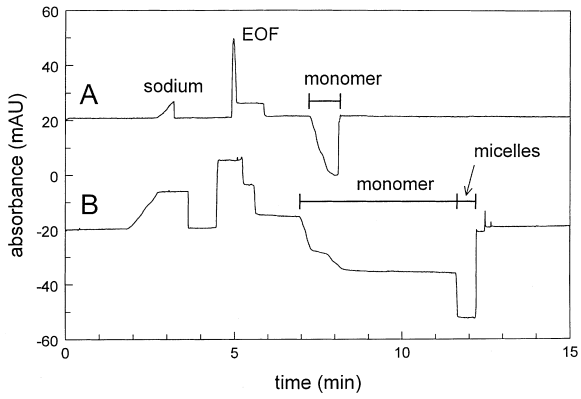

Fig. 4. Indirect UV detection of the surfactant zone in PF-MEKC with MES as visualizing agent. Electrolyte system: 50 m*M* Tris–MES (pH 8.5); surfactant zone: 25 m*M* SDS in run buffer, zone injection: (A) 10 kV, 10 s and (B) 10 kV, 120 s; detection wavelength, 200 nm.

mobility is higher than that of the co-ion. According to the electroneutrality condition, the concentration of the UV-absorbing counter ion of the background electrolyte will also be higher, resulting in a positive UV peak for the non-UV-absorbing sample compound. The DS surfactant zone can be observed as a large negative dip. From the migration times of the front and the rear side of this dip it can be calculated that the length of the DS zone is ~6.6 cm. This is much longer than would be expected from a short 10-s injection. In addition, the effective mobility, calculated from the rear side of the dip, is $-23.13 \cdot 10^{-5}$ cm^2/V s. This value is much closer to the effective mobility of individual DS ions than to the effective mobility of DS micelles (see Table 1). These results demonstrate that the injected DS molecules are migrating as surfactant monomers for the main part of the analysis time and not as micelles.

The underlying mechanism for this phenomenon is schematically presented in Fig. 5. Due to their higher effective mobility, DS micelles will migrate more slowly than DS monomers in the injected surfactant zone. After a short time two parts can be distinguished in the surfactant zone, i.e. part A containing only surfactant monomers and part B containing both surfactant monomers and micelles. The surfactant concentration in part A is at or below the critical micelle concentration (CMC) and consequently no micelles can be formed. These ions will migrate with a low effective mobility for the remaining analysis time. Micelles that migrate into the buffer at the rear side of the surfactant zone experience an aqueous phase without surfactant monomers. According to the equilibrium condition the micelle concentration will decrease to provide the aqueous phase with surfactant monomers. This process continues during the analysis, resulting in an increase of part A and a decrease of part B. The total amount of micelles will gradually decrease and finally a steady state is reached where all surfactant molecules are migrating as monomers. Consequently a much longer surfactant zone is obtained with a lower concentration than originally injected. The required time to reach this steady state is longer for longer injected zones or for zones with a higher surfactant concentration.

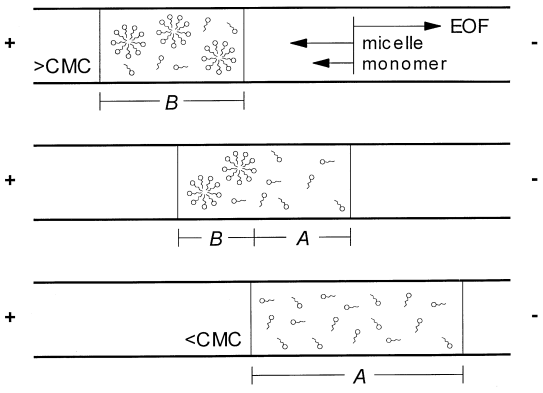

Fig. 5. Schematic representation of the migration behaviour of SDS micelles under PF-MEKC conditions. Part B contains both DS micelles and monomers, part A contains only DS monomers. Micelles break down during the analysis due to differences in the effective mobility of DS micelles and DS monomers, resulting in a longer zone with a lower surfactant concentration. For further explanation, see text.

The above described phenomenon will not be encountered with neutral surfactants [8] or high-molecular-mass surfactants [6] since neutral surfactants possess no electrophoretic mobility whereas high-molecular-mass surfactants generally have CMC values close or identical to zero.

In Fig. 4B the electropherogram is shown for the electrokinetic injection (10 kV, 120 s) of 25 m*M* SDS, dissolved in background electrolyte. Here a small part of the surfactant zone is still migrating as micelles. Due to the higher DS concentration in this part of the zone a more negative UV signal is obtained. From the rear side of the dip an effective mobility of $-33.05 \cdot 10^{-5}$ cm^2/V s is calculated. Since micelles continuously break down at the rear side of the surfactant zone, this value is somewhat lower than the effective mobility of DS micelles listed in Table 1. The influence of the surfactant concentration in the injected zone is illustrated in Fig. 6. For a two-fold increase in surfactant concentration and a two-fold increase in injection time comparable zone lengths are obtained. These results demonstrate that the final zone length is determined rather by the total injected amount of surfactant than by the injected zone length.

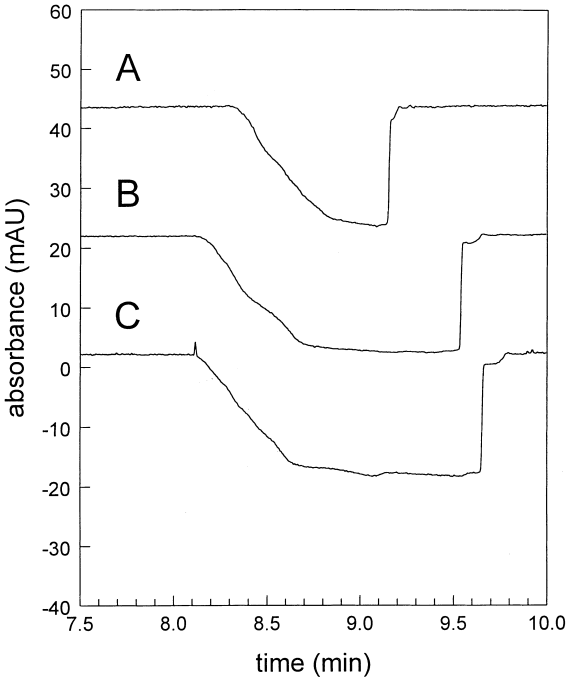

Fig. 6. UV signal obtained with indirect UV detection for different compositions of the surfactant zone. Electrolyte system: 50 m*M* Tris–MES (pH 8.5). Surfactant zone: (A) 25 m*M* SDS, injection 10 kV, 10 s; (B) 25 m*M* SDS, injection 10 kV, 20 s; (C) 50 m*M* SDS, injection 10 kV, 10 s; detection wavelength, 200 nm.

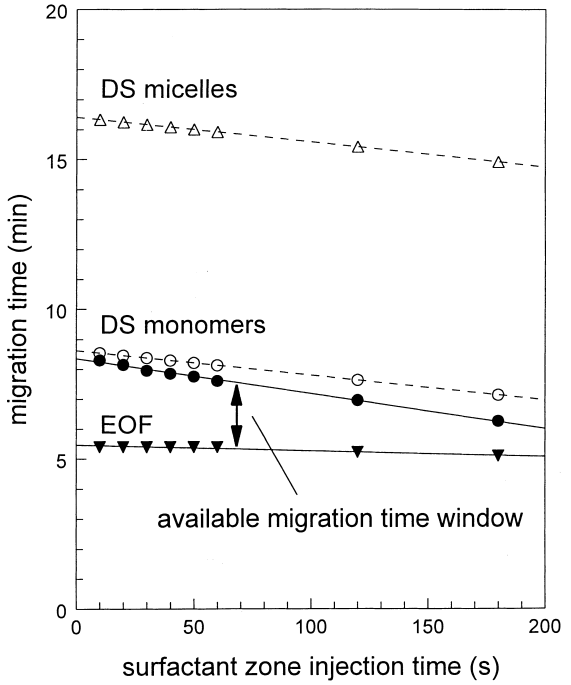

Fig. 7. Available migration time window as a function of the surfactant zone injection time. Solid lines represent measured values, dotted lines represent calculated values, respectively. Electrolyte system: 50 m*M* Tris–MES (pH 8.5).

4.2. Partial-filling MEKC

4.2.1. Available migration time window

The typical behaviour of the surfactant zone will have a pronounced effect on the performance of PF-MEKC experiments. The available migration time window, i.e. the time between the EOF and the front of the surfactant zone, is determined by the length of the injected surfactant zone, the electroosmotic mobility and the effective mobility of surfactant monomers. In Fig. 7 measured migration times of the front of the surfactant zone, determined by indirect UV detection, and the EOF are shown as a function of the zone injection time. As expected a decrease of the available migration time window is obtained with increasing zone lengths. In Fig. 7 also calculated values are shown, using the effective mobilities of DS monomers and DS micelles listed in Table 1. Due to the low effective mobility of DS monomers, the actual available migration time window is much smaller than would be expected based on the high effective mobility of DS micelles. The small difference in measured and calculated migration times of DS monomers may be attributed to differences in the electric field strength in the surfactant zone and the buffer due to different ionic strengths, which are not taken into account in the calculations.

4.2.2. Influence of surfactant concentration and zone length

Since the separation of sample compounds in PF-MEKC is based on differences in micellar solubilization, separation will only occur in part B of the surfactant zone. Since the length of part B decreases with time, compounds with a higher retention factor

will experience a smaller effective separation length. However, the decrease of part B is linear with time and, consequently, still a linear relationship may be expected between the migration time and the injected zone length for a given retention factor. To investigate the influence of the surfactant concentration and the zone length on migration times in PF-MEKC, experiments were carried out with a sample mixture of acetophenone, propiophenone and butyrophenone, and surfactant solutions containing 25, 50 and 100 m*M* SDS, respectively. In order to monitor the surfactant zone by indirect UV detection, an electrolyte system of 50 m*M* Tris adjusted to pH 8.5 by adding MES was applied. In Fig. 8 all measured migration times of the sample compounds and the front side of the surfactant zone (both part A and part B, if present) are shown. Linear relationships are obtained between migration time and zone length for all compounds at each surfactant concentration. As expected, larger differences in migration times are obtained for higher zone lengths and for higher surfactant concentrations. With the 50 and 60 s injection of the 50 m*M* SDS solution, butyrophenone migrates in part A of the surfactant zone. With the 40, 50 and 60 s injection of the 100 m*M* SDS solution it could be observed that micelles are still present. For the 50 and 60 s injection, butyrophenone migrates in part B of the surfactant zone and is detected before it is retained for the full time. As a result these migration times are lower than the linear graph.

The results in Fig. 8 suggest that comparable migration times can be obtained by different combinations of zone length and surfactant concentration. However, at the micelle zone–buffer boundary an additional band broadening mechanism occurs as described in Section 4.2.3 Since this additional band broadening increases with higher retention factors, a low surfactant concentration is to be preferred.

4.2.3. Efficiency in PF-MEKC

In Table 2 theoretical plate numbers are shown for the three alkyl aryl ketones obtained with different surfactant concentrations in normal MEKC and PF-MEKC, respectively. Lower efficiencies are obtained with PF-MEKC in all experiments. Moreover, a decrease in efficiency is observed in PF- MEKC with an increase in retention factor, i.e. for stronger retained compounds and for higher surfactant concentrations. These differences in efficiency are main-

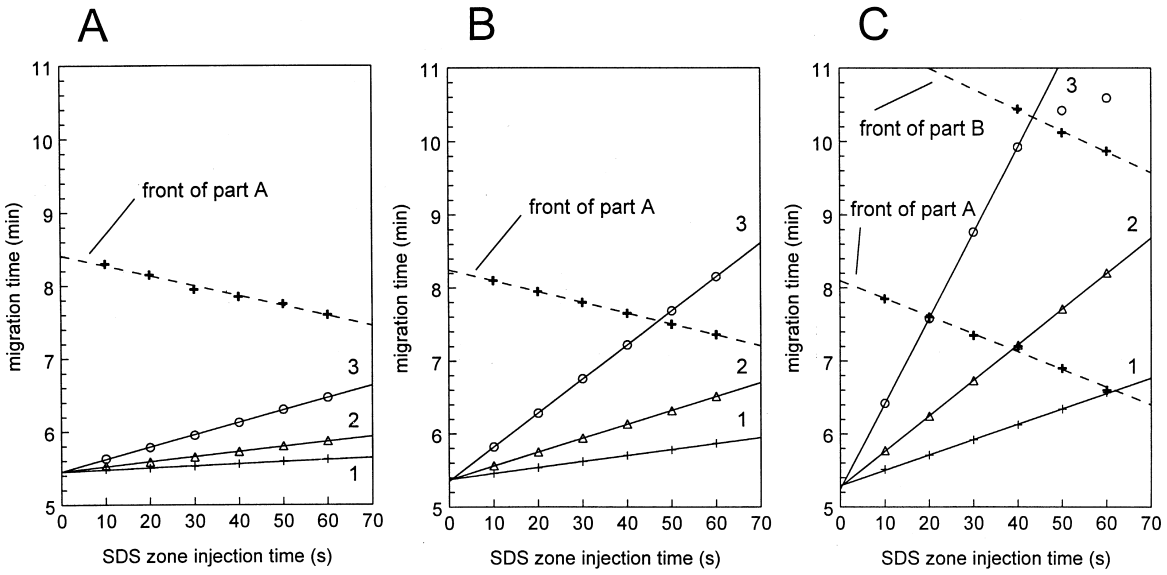

Fig. 8. Measured migration times of (1) acetophenone, (2) propiophenone and (3) butyrophenone in PF- MEKC as a function of the SDS zone injection time. Electrolyte system: 50 m*M* Tris–MES (pH 8.5); surfactant zone: (A) 25 m*M*, (B) 50 m*M* and (C) 100 m*M* SDS, respectively. The fronts of part A and part B of the surfactant zone were determined by indirect UV detection at a wavelength of 200 nm.

Table 2
Theoretical plate numbers, N (/1000), and retention factors, k, for three alkyl aryl ketones obtained with different surfactant concentrations in normal MEKC and PF-MEKC

Operational mode	Compound	Concentration SDS (mM)					
		25		50		100	
		N	k	N	k	N	k
Normal MEKC	Acetophenone	278	0.76	306	1.79	259	3.51
	Propiophenone	314	1.65	342	4.14	274	7.99
	Butyrophenone	321	3.96	265	12.22	215	21.53
PF-MEKC	Acetophenone	178		179		123	
	Propiophenone	192		152		54	
	Butyrophenone	156		48		12	

Sample concentration, 0.05 μl/ml; sample solution: 25 mM SDS in water + 10% (v/v) MeOH.
Electrolyte system: 50 mM Tris–MES (pH 8.5). Normal MEKC: 25 mM SDS; PF-MEKC: 25 mM SDS, surfactant zone injection, 10 kV for 20 s.

ly due to an additional band broadening mechanism in PF-MEKC. The overall velocity of an analyte in part B of the surfactant zone, ν_B, is given by:

$$\nu_B = \frac{1}{1+k}\nu_{EOF} + \frac{k}{1+k}(\nu_{MC} + \nu_{EOF}) \quad (9)$$

The velocity in part A of the surfactant zone is equal to the electroosmotic velocity, ν_{EOF}. Consequently an analyte zone obtains a higher velocity if it passes the boundary between part A and B in the surfactant zone, resulting in broadening of the analyte zone. From Eq. (9) it can be concluded that this effect will be stronger for high retention factors. In order to investigate this band broadening mechanism in more detail, PF-MEKC experiments were carried out in a short capillary of 8.5-cm effective length. For these experiments the original outlet side of the capillary in the HP^{3D}CE instrument was used as inlet side and a negative voltage was applied. Samples were introduced by electrokinetic injection with −5 kV for 5 s. With this set-up it is possible to detect the analytes while they are still migrating in part A or part B of the surfactant zone. In Fig. 9 the electropherograms are shown for 40- and 50-s injections of a 25 mM SDS solution, respectively. In Fig. 9A all compounds are migrating in part A of the surfactant zone. In Fig. 9B acetophenone and propiophenone are migrating in part A, whereas butyrophenone is migrating in part B of the surfactant zone. Although the migration time is longer, a much better peak shape is obtained for butyrophenone. The difference in peak height for butyrophenone between the 40- and 50-s injection in the 8.5-cm capillary clearly illustrates the additional band broadening mechanism in PF-MEKC when an

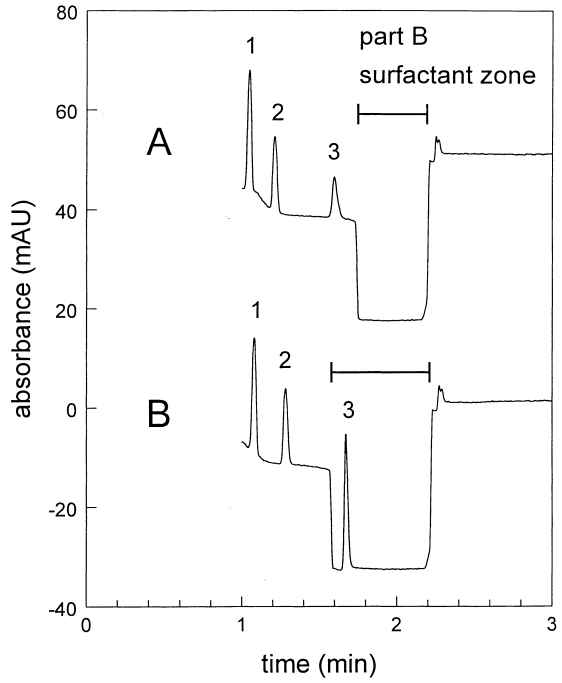

Fig. 9. Electropherograms of (1) acetophenone, (2) propiophenone and (3) butyrophenone obtained by PF-MEKC with a short capillary of 8.5 cm effective length. Electrolyte system: 50 mM Tris–MES (pH 8.5); surfactant zone: 25 mM SDS, injection (A) −10 kV, 40 s, (B) −10 kV, 50 s; detection wavelength, 200 nm; electrokinetic injection: −5 kV, 5 s.

analyte passes the micelle zone–buffer boundary. In addition to the above described mechanism, differences in the electroosmotic flow and the electric field strength between the surfactant zone and the buffer may also contribute to extra band broadening in PF-MEKC [16].

4.3. On-line partial filling MEKC–MS

The possibilities of PF-MEKC for the on-line coupling with MS were investigated for the separation and identification of several pharmaceuticals. In Fig. 10 electropherograms are shown for a sample mixture of five pharmaceuticals, obtained with (A) normal MEKC and (B to D) PF-MEKC applying different surfactant zones. Due to the limitations mentioned in Section 4.2 it is not possible to obtain a complete separation of all five compounds before the surfactant zone with PF-MEKC. Based on these results caffeine and ethenzamide were selected as test compounds for on-line PF-MEKC–MS. For these compounds it is possible to obtain a baseline separation before the surfactant zone reaches the MS. For these experiments an electrolyte system of 20 m*M* ammonium acetate adjusted to pH 10 with NaOH was applied. With electrokinetic injection of the surfactant zone, the process where micelles break down will also occur during the injection of the zone. This is unfavourable with respect to the available migration time window. Therefore in these PF-MEKC–MS experiments the surfactant zone was introduced by pressure injection so that the whole surfactant zone still contains micelles at the start of the separation.

In Fig. 11 the selected ion chromatograms and the corresponding UV electrokinetic chromatogram of caffeine and ethenzamide are shown. A broader peak is obtained for ethenzamide, due to the additional band broadening mechanism described in Section 4.2.3. From experiments in the negative-ion mode the DS zone was found to migrate after the sample compounds at ~23 min which is in agreement with the migration time calculated from the electroosmotic mobility and the effective mobility of DS monomers. In Fig. 12 the reconstructed ion chromatograms and the corresponding mass spectra are shown, obtained in the full scan mode. For these experiments a long injection of 30 s was applied to ensure that the sample zones were long enough to obtain sufficient spectral data. The strongest signal for ethenzamide ($M=165.19$) was obtained at $m/z=149$. This is probably due to the loss of the amine group during the ionisation process. Satisfactory mass spectra were obtained for both compounds with the APCI interface. However, here it should be mentioned that the sample concentration of 0.5 mg/ml is rather high. In Fig. 13 the migration times of caffeine and ethenzamide obtained at different days are shown. The reproducibility was rather low, as indicated by the relative standard deviations (R.S.D. %) of 8.5 and 7.0 for caffeine and ethenzamide, respectively. This may be attributed to the low buffer capacity of the applied electrolyte system. These results clearly demonstrate that although the separation performance of PF-MEKC is limited, this technique provides a possible way for the on-line coupling of MEKC–MS.

5. Conclusions

From the foregoing paragraphs it can be concluded that with PF-MEKC a separation is possible based on micellar solubilization, whereas the surfactant does not reach the detector. However, several severe limitations can be recognised compared to normal MEKC. First, the total separation volume is smaller due to the relative short surfactant zone. Second, the migration time window in PF-MEKC is smaller since it is determined by the effective mobility of surfactant monomers and not by the effective mobility of micelles as in normal MEKC. Third, an extra band broadening mechanism occurs at the micelle zone–buffer boundary resulting in a lower efficiency. As a result of these limitations, a lower resolution is obtained in PF-MEKC compared to normal MEKC.

Despite these limitations, PF-MEKC provides a possible way for the on-line coupling of MEKC–MS. Separated sample compounds can be detected before the surfactant zone reaches the MS. Hence the negative effect of non-volatile surfactant molecules on the ionisation process is eliminated and good mass spectra are obtained.

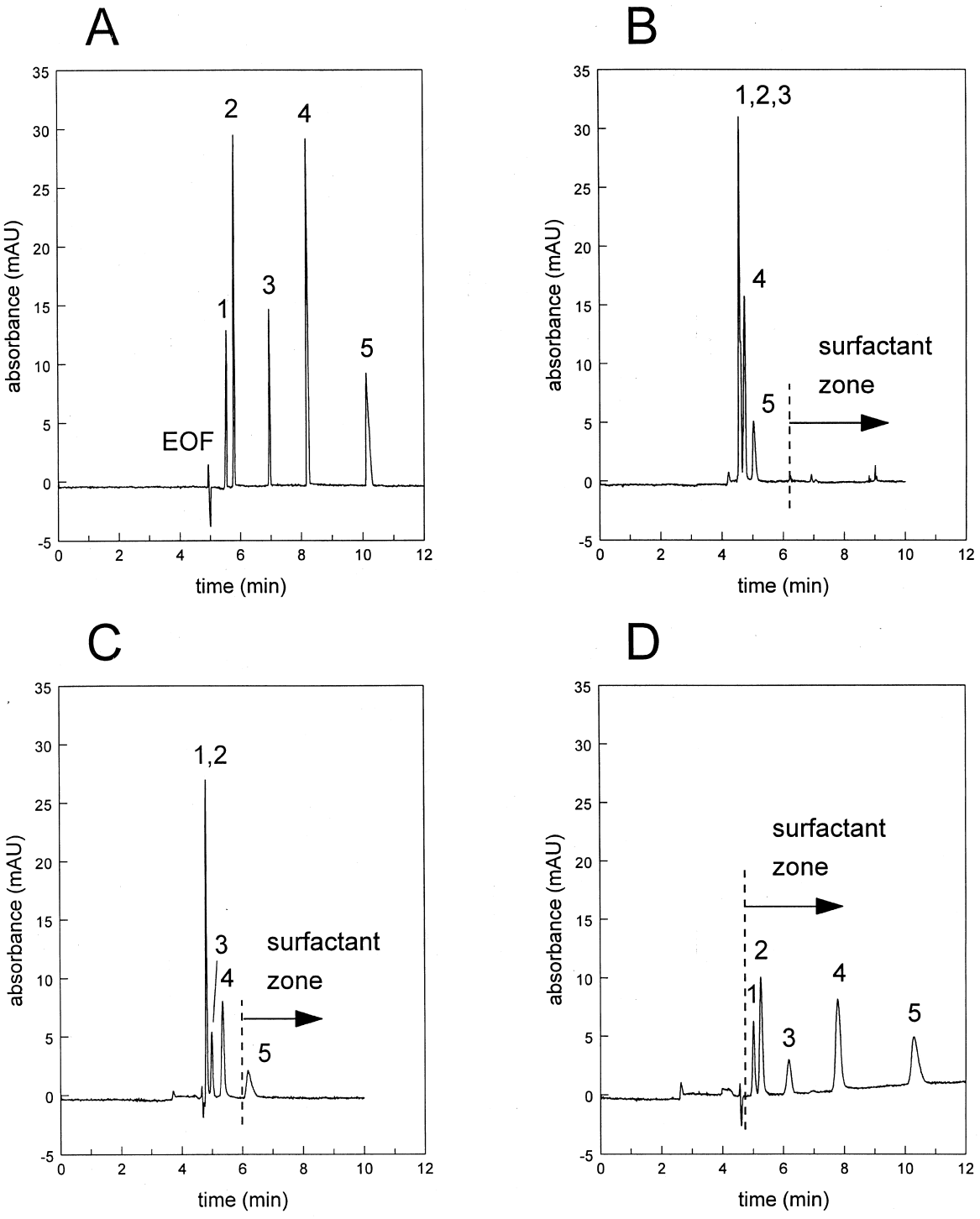

Fig. 10. Electropherograms of (1) acetaminophen, (2) caffeine, (3) guaifenisin, (4) ethenzamide and (5) isopropylantipyrine obtained by (A) normal MEKC and (B–D) PF-MEKC. Electrolyte system: 20 m*M* Tris–phosphate (pH 8.5); normal MEKC: 25 m*M* SDS; PF-MEKC: (B and C) 25 m*M* and (D) 50 m*M* SDS dissolved in background electrolyte; surfactant zone injection: (B) 10 kV, 40 s, (C) 10 kV, 120 s, (D) 10 kV, 240 s; detection wavelength, 214 nm.

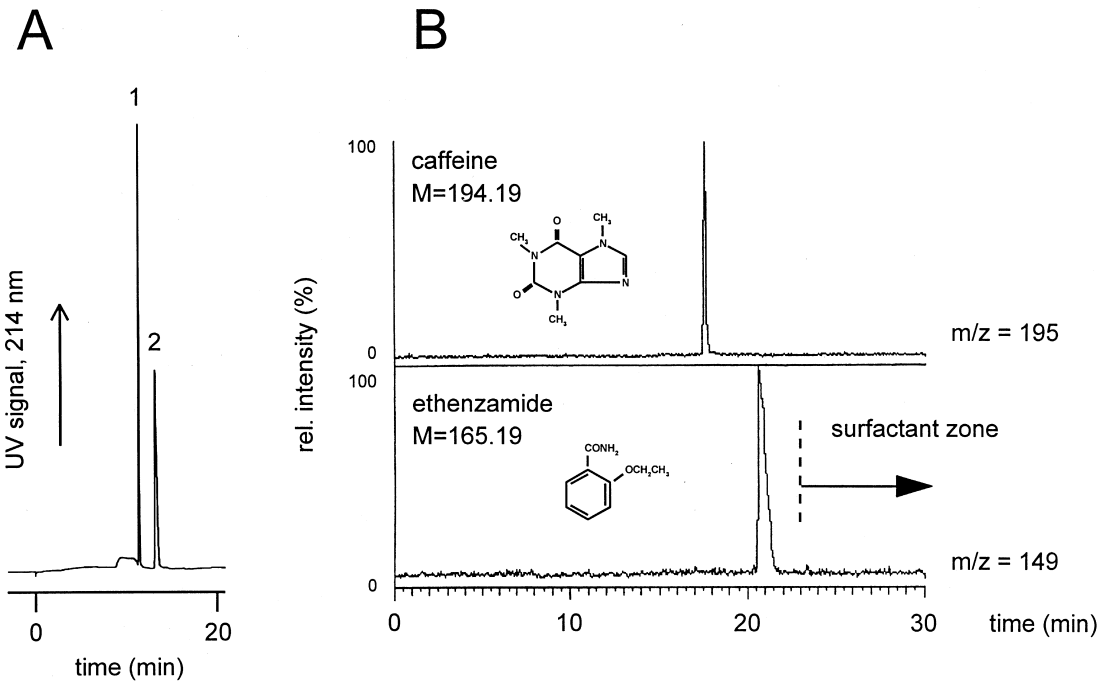

Fig. 11. (A) UV signal and (B) selected ion chromatograms for (1) caffeine and (2) ethenzamide obtained by on-line PF-MEKC–MS. Sample concentration: 0.5 mg/ml; buffer, 20 m*M* ammonium acetate (pH 10); surfactant zone: 25 m*M* SDS in background electrolyte; zone injection: 200 mbar, 1 min; sample injection: 50 mbar, 6 s; capillary: 100 cm×50 μm I.D.; UV detection at 65 cm; inlet voltage, 18 kV; electrospray, 3 kV.

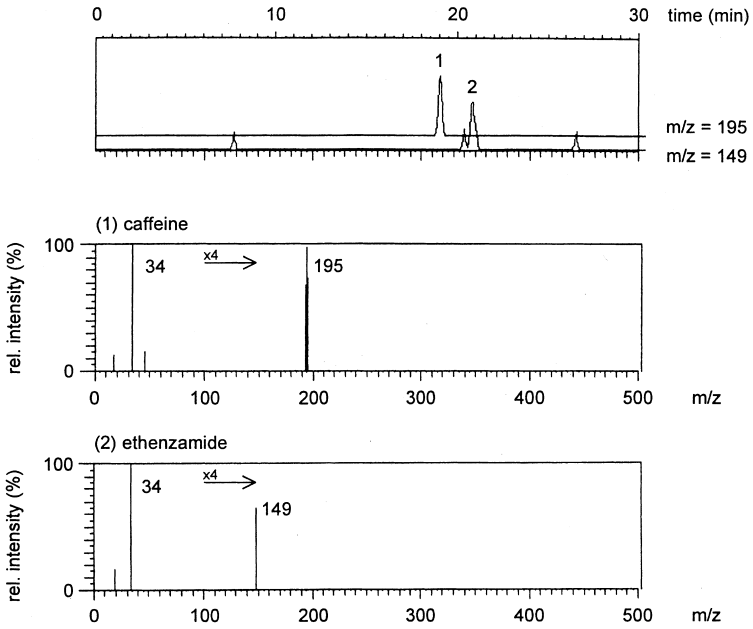

Fig. 12. Reconstructed ion chromatograms and mass spectra for (1) caffeine and (2) ethenzamide. Conditions are the same as in Fig. 11 except for the sample injection time which is 30 s.

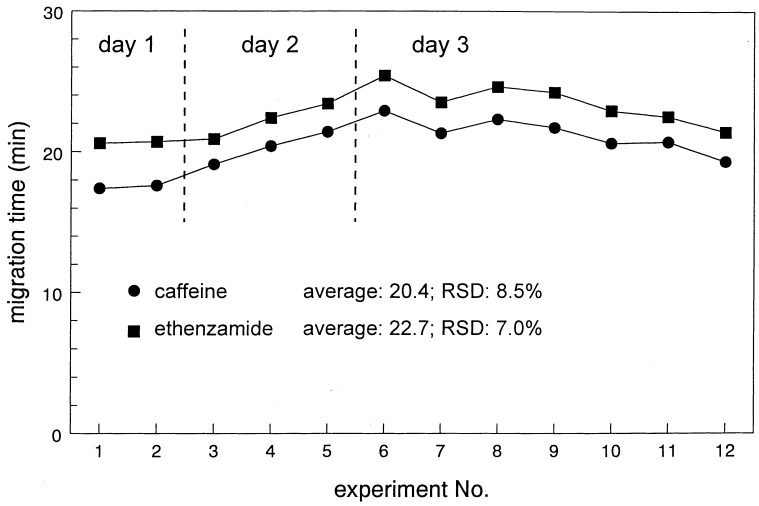

Fig. 13. Reproducibility of migration times with PF-MEKC–MS for caffeine and ethenzamide. Conditions are the same as in Fig. 11.

Acknowledgements

The authors wish to express their gratitude to the Japan Society for the Promotion of Science (JSPS) for funding a postdoctoral fellowship (No. 99096) and to the Japan Ministry of Education, Science and Culture for a grant-in-aid (No. 99096).

References

[1] W.M.A. Niessen, U.R. Tjaden, J. van der Greef, J. Chromatogr. 636 (1993) 3.
[2] K.L. Rundlett, D.W. Armstrong, Anal. Chem. 68 (1996) 3493.
[3] Y. Takada, M. Sakairi, H. Koizumi, Anal. Chem. 67 (1995) 1474.
[4] Y. Takada, M. Sakairi, H. Koizumi, Rapid Commun. Mass Spectrom. 9 (1995) 488.
[5] M.H. Lamoree, U.R. Tjaden, J. van der Greef, J. Chromatogr. A 712 (1995) 219.
[6] H. Ozaki, N. Itou, S. Terabe, Y. Takada, M. Sakairi, H. Koizumi, J. Chromatogr. A 716 (1995) 69.
[7] W.M. Nelson, Q. Tang, A. Kamel Harrata, C.S. Lee, J. Chromatogr. A 749 (1996) 219.
[8] K. Koezuka, H. Ozaki, N. Matsubara, S. Terabe, J. Chromatogr. B 689 (1997) 3.
[9] L. Yang, A. Kamel Harrata, C.S. Lee, Anal. Chem. 69 (1997) 1820.
[10] H. Nishi, S. Terabe, J. Chromatogr. A 735 (1996) 3.
[11] P.G. Muijselaar, K. Otsuka, S. Terabe, J. Chromatogr. A 780 (1997) 41.
[12] S. Terabe, K. Otsuka, K. Ichikawa, A. Tsuchiya, T. Ando, Anal. Chem. 56 (1994) 113.
[13] S. Terabe, K. Otsuka, T. Ando, Anal. Chem. 57 (1985) 834.
[14] L. Valtcheva, J. Mohammed, G. Petterson, S. Hjertén, J. Chromatogr. 638 (1993) 263.
[15] Y. Tanaka, S. Terabe, J. Chromatogr. A 694 (1995) 277.
[16] W.M. Nelson, C.S. Lee, Anal. Chem. 68 (1996) 3265.
[17] D. Attwood, A.T. Florence, Surfactant Systems, Chapman and Hall, New York, 1983.